Silicon Quantum Dots

DOI: 10.1002/anie.200802230

Ultrastable, Highly Fluorescent, and Water-Dispersed Silicon-Based Nanospheres as Cellular Probes**

Yao He, Zhen-Hui Kang, Quan-Song Li, Chi Him A. Tsang, Chun-Hai Fan, and Shuit-Tong Lee**

Fluorescent cellular probes are powerful tools for studying cellular morphology, behavior, and physiological functions. For optimum imaging and tracking of biological cells, these probes should be water-dispersible, antibleaching, luminescent, and biocompatible.[1] In the last century, organic dyes and fluorescent proteins were mostly used as fluorescent probes in biological and biomedical research; however, they suffer from severe photobleaching that restricts their applications for long-term in vitro or in vivo cell imaging.[2] This shortcoming has led to an intense interest in colloidal fluorescent semiconductor quantum dots (QDs) since II/VI QDs were shown to be promising for cell imaging in 1998.[3] Compared to fluorescent dyes, QDs possess unique advantages such as size-tunable emission wavelengths, broad photoexcitation, narrow emission spectra, strong fluorescence, and high resistance to photobleaching.[4] Consequently, QDs have been widely used as a new class of fluorescent probes in cellular research, for example, in vitro imaging, cell labeling, and tracking cell migration.[5] However, recent investigations have shown that these QDs are cytotoxic, especially under harsh conditions (e.g., UV irradiation),[6] because heavy metal ions (such as Cd or Pb ions) are often released in oxidative environments, which leads to severe cytotoxicity by conventional mechanisms of heavy metal toxicity.[7] Surface modification of QDs, such as epitaxial growth of the ZnS shell, silica coating, or polymer coating, has been used to alleviate the cytotoxicity problem.[8] While these techniques are viable to a certain extent, they are relatively complicated and require additional processing steps. Notably, the risk of cytotoxic problems still remains since heavy-metal ions contained in the modified QDs may invariably be released in physiological environments.[9] Consequently, the inherent problems, that is, severe photobleaching and cytotoxicity, associated with the traditional dyes and the fluorescent II/VI QDs remain unsolved, and have fueled a continual and urgent search for new cellular probes that are more photostable and biocompatible.

Silicon is the leading semiconductor material for technological applications because of its wide-ranging applications by the electronics industry. Silicon-based nanostructures, such as nanoribbons, nanowires, and nanodots, are being intensely investigated.[10] The quantum confinement phenomenon in silicon QDs (SiQDs) is a particular focus of research since it would increase the probability of irradiative recombination by indirect-to-direct band-gap transitions, which lead to enhanced fluorescent intensity and the prospect of long-awaited optical applications.[11] The biocompatibility and noncytotoxic properties of SiQDs are much better than those of traditional II/VI QDs, although their photoluminescence (PL) intensity is weaker.[12] As such, silicon-containing materials may be useful for biological applications such as cellular imaging and labeling because of their favorable biocompatibility, if water-dispersed silicon nanomaterials with adequate stability and strong fluorescence are properly developed. Herein we report a new variety of silicon-based nanospheres for use as cellular probes, which possess excellent water-dispersibility, strong photoluminescence, and robust photostability.

Our design of these nanospheres was formulated from calculations performed by using the B3LYP/6-31G method, a classic calculation method based on hybrid density functional theory. Figure 1a shows that the calculated free energy of the products P_{Si-O} (-15.2 kcal mol^{-1}) is higher than that of P_{Si-C} (-33.1 kcal mol^{-1}), whereas the energy barrier of forming the Si–O bond ($E_{Si-O} = 41.5$ kcal mol^{-1}) is much lower than that of the Si–C bond ($E_{Si-C} = 59.5$ kcal mol^{-1}). The energy consideration implies that an acrylic acid monomer (AAc) would react with the surface of the SiQDs via the carbonyl or alkene groups by forming Si–O or Si–C bonds, as previously reported.[13] Furthermore, the calculations yield the energy relation of E_{Si-O} (41.5 kcal mol^{-1}) $< E_{blue}$ (58.3 kcal mol^{-1}) $< E_{Si-C}$ (59.5 kcal mol^{-1}) $< E_{UV}$ (79.4 kcal mol^{-1}). It shows that the energy value of blue light (E_{blue}) is larger than the energy barrier of formation E_{Si-O} of the Si–O bond, but less than the

[*] Prof. C.-H. Fan
Shanghai Institute of Applied Physics
Chinese Academy of Sciences
Shanghai 201800 (P.R. China)
E-mail: fchh@sinap.ac.cn
Dr. Y. He, Dr. Z.-H. Kang, Q.-S. Li, C. H. A. Tsang, Prof. S.-T. Lee
Center of Super-Diamond and Advanced Films (COSDAF) and
Department of Physics and Materials Science
City University of Hong Kong
Hong Kong SAR (P.R. China)
Fax: (+852) 2-784-4696
E-mail: apannale@cityu.edu.hk
Dr. Y. He, Dr. Z.-H. Kang
Functional Nano & Soft Materials Laboratory (FUNSOM)
Soochow University, Suzhou, 215123 Jiangsu, China

[**] This work was supported by the Research Grants Council of Hong Kong (No. CityU 101608 and CityU 101807), 863 project (2006AA03Z302), and the National Basic Research Program of China (2006CB93000, 2007CB936000). We thank Prof. L. H. Wang for fruitful discussions and generously supplying CdTe and CdTe/CdS/ZnS quantum dot samples and Dr. C. W. L. Michael, H. T. Lu, and Y. Y. Su for their technical assistance.

Supporting information for this article (including experimental details) is available on the WWW under http://dx.doi.org/10.1002/anie.200802230.

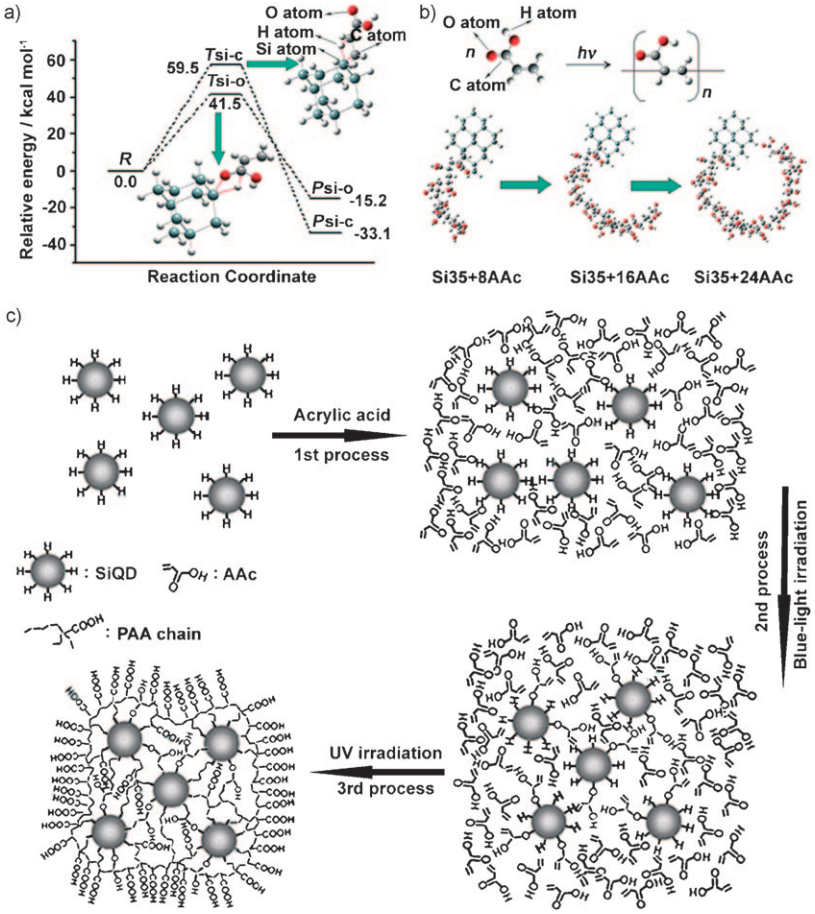

Figure 1. a) Schematic representation showing potential energy profiles for Si–C and Si–O bond formation along with B3LYP/6-31G relative energies (kcal mol^{-1}) of the reactants (*R*), transition states (*T*), and products (*P*). Red lines indicate the new Si–C, Si–O, Si–H, and C–H bonds in the addition reaction. b) Optimized structures involved in the formation of the PAA chain on the surface of the SiQD. c) Schematic representation showing the synthesis of silicon-based nanospheres. The whole process was performed in an N_2 atmosphere. To simplify the model, only five SiQDs are shown in one nanosphere.

$E_{Si\text{-}C}$ value of the Si–C bond; whereas the energy value of UV light (E_{UV}) is substantially larger than $E_{Si\text{-}C}$, which indicates that the Si–O bond or Si–C bond is likely to form under blue ($\lambda_{blue} = 490$ nm) or UV ($\lambda_{UV} = 360$ nm) irradiation, respectively. In contrast, alkenes are prone to undergo self-addition reactions to form long poly(acrylic acid) (PAA) chains, especially under UV irradiation.[14] Furthermore, the optimized structure shows that the PAA chain on the surface of a SiQD tends to grow into a ring, rather than a straight line, with increasing chain length, since the ring structure is energetically the most favorable conformer (Figure 1b). Therefore, once the PAA chain is formed, different SiQDs will be linked together by these chains by the formation of Si–O or Si–C bonds; this results in a silicon-based nanosphere.

On the basis of the above analysis and our previous theoretical studies,[15] we developed a new strategy for the synthesis of fluorescent, size-controllable silicon nanospheres. These nanospheres can be readily produced in three consecutive steps (Figure 1c). In the first step, hydrogen-terminated SiQDs were prepared by using the electrochemical method recently developed by our research group.[16] Afterwards, a precursor mixture was obtained by adding AAc to a SiQD dispersion in ethanol under continuous magnetic stirring. In the second step, the mixture was irradiated with blue light to promote the reaction of SiQDs with AAc by Si–O bond formation. In the third step, hydrosilylation and addition reactions of AAc were initiated by UV irradiation to induce eventual formation of the nanospheres. The UV irradiation time in the third step is critical for controlling the size distribution of nanospheres. Under UV irradiation, the alkene in the polymer chain and the residual AAc monomers will continually react to produce PAA with a high degree of polymerization, which leads instead to the formation of the SiQDs-PAA colloidal complex. Notably, besides the fluorescent Si nanospheres, we expect that Si nanospheres with multiple functions may be similarly prepared by this novel strategy (e.g., we have prepared magnetic and fluorescent Si nanospheres by using this approach (data not shown).)

Figure 2 displays transmission electron microscopy (TEM) images that show the size distributions of the as-prepared nanospheres. Figure 2a and b show clearly that the nanospheres are spherical in shape and highly monodisperse. Indeed, the size distribution (Figure 2c) of over 350 nanospheres yields an average size and standard deviation (SD) of (59.4 ± 8.5) nm, and the polydispersity (PD, or the relative standard deviation) of 14.3%. Importantly, Si nanospheres of different sizes can be conveniently prepared by varying the irradiation time in the third step. Figure 2d–f shows the TEM images and size distribution of nanospheres with an average size of (121.3 ± 12.7) nm and PD of 12.7%, while Figure 2g–i shows the nanospheres with an average size of 206.9 nm and PD value of 9.2%. Figure 3a displays TEM images of three nanospheres with diameters of approximately 59, 121, and 207 nm, which contain approximately 170, 500, and 950 SiQDs, respectively; this further demonstrates that nanospheres of controllable sizes can be produced using the new strategy. Moreover, the corresponding hydrodynamic-diameter distributions of the nanospheres in water measured by dynamic light scattering (DLS) are shown in Figure 3b, giving average hydrodynamic diameters of 70, 137, and 231 nm, respectively. The small deviation in diameter measured by TEM and DLS could be attributed to different surface states of the as-prepared nanospheres in the aqueous phase.[17] The high-resolution TEM image in Figure 3c shows the SiQDs inside the nanosphere have the characteristic silicon crystal lattice and high crystallinity, revealing that SiQDs preserve the original structural properties of silicon.

Nonmodified SiQDs usually have a low PL quantum yield (PLQY) because of the indirect band gap of silicon.[11] In

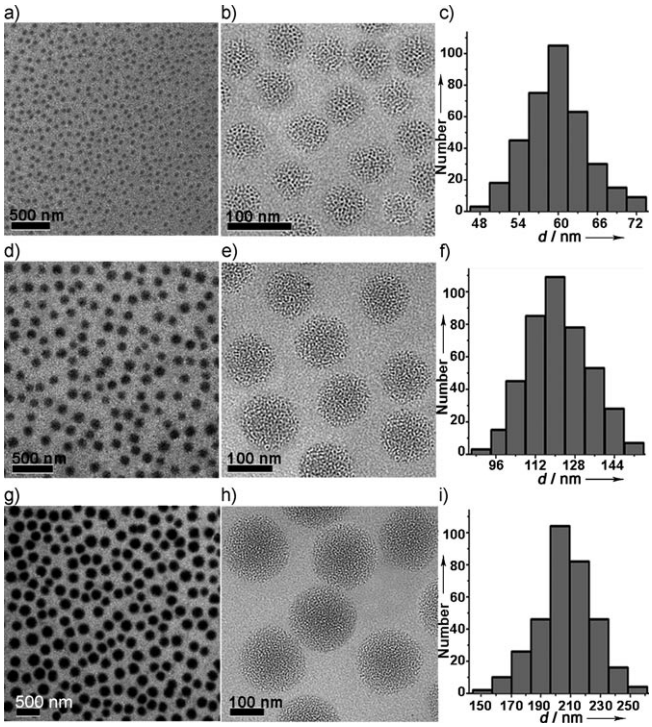

Figure 2. Transition electron microscopy (TEM) images and the size distribution of the as-prepared nanospheres. a, b) TEM images of the nanospheres with a size of approximately 60 nm, and c) the corresponding size distribution. d, e) TEM images of the nanospheres with a size of approximately 120 nm, and f) the corresponding size distribution. g, h) TEM images of the nanospheres with a size of approximately 210 nm, and i) the corresponding size distribution.

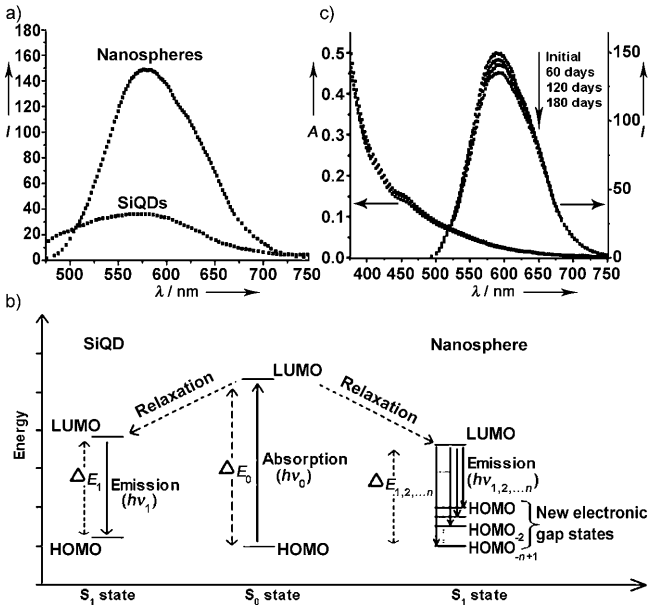

Figure 4. a) Photoluminescence spectra of the nonmodified SiQDs and as-prepared nanospheres. To ensure an objective comparison, the samples of SiQDs and nanospheres were directly extracted respectively from the original solution in the initial or the final state of the whole process shown in Figure 1c. Neither sample received any post-treatment. b) Schematic diagram showing photoabsorption and emission process for the free-standing SiQDs and the nanosphere. c) Temporal evolution of absorption and corresponding PL spectra of the as-prepared nanospheres over 180 days in air and under ambient conditions without any special protection.

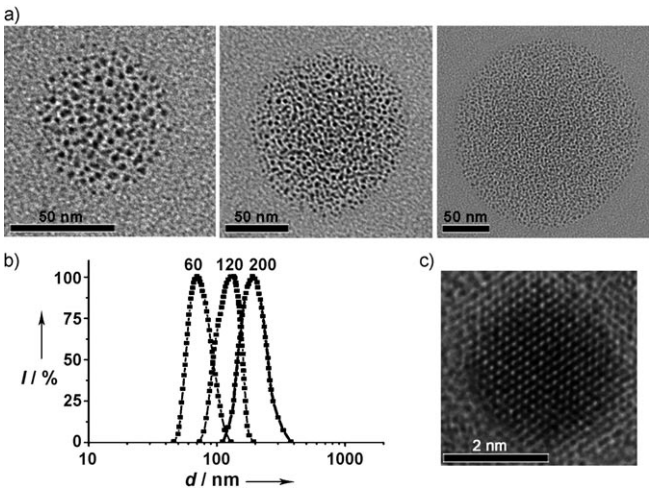

Figure 3. a) TEM images of three nanospheres with approximate sizes of 60 nm (left), 120 nm (middle), and 200 nm (right). b) Representative dynamic-light-scattering histogram of the nanospheres with approximate sizes of 60 nm, 120 nm, and 200 nm. c) HRTEM image of a single SiQD inside the as-prepared nanospheres.

contrast, the PAA-modified nanospheres have a PLQY of 15–20%, which is more than six times larger than the PLQY of SiQDs in the free state (2–3%). The PLQY of the two samples are compared in Figure 4a, which illustrates that the nanosphere solution (right) shows a distinctly higher PL intensity than the original SiQDs solution (left), with a slightly red-shifted wavelength. Theoretical calculations reveal that many new gap states are indeed generated in the nanospheres relative to the nonmodified SiQDs (Figure 4b).[15a] Thus, a large amount of electrons are transferred from the lowest unoccupied molecular orbitals (LUMOs) to the new states, that is, highest occupied molecular orbitals ($HOMO_{0,-1,-2...}$), with a narrower HOMO–LUMO energy gap, thereby leading to a significant enhancement of PL intensity and a slight red-shift. It is widely recognized that poor PL stability is a major barrier to the wide applications of nanostructured silicon. Significantly, our nanospheres were remarkably stable during long-term observation. After storage in air for 180 days without any additional protection, 90% of the initial PL intensity was maintained (Figure 4c). This is in sharp contrast to unmodified SiQDs, which suffered from severe PL quenching in several hours.[12a] The remarkable PL stability is attributed to the polymer chains, which act as a protective shell around the SiQDs, thus shielding the SiQD surface from molecular quenching and oxidation. Consequently, these fluorescent nanospheres of controllable sizes and excellent stability can enable application possibilities in long-term cell labeling and monitoring.

To establish their utility as cellular probes, we used the as-prepared nanospheres as fluorophores to label HEK293T human kidney cells. The resulting sample, imaged by laser-

scanning confocal fluorescence microscopy (LSCFM), showed that the photoluminescence of the nanosphere-labeled HEK293T cells is intense and clearly spectrally resolved (Figure 5a). Furthermore, luminescent signals of

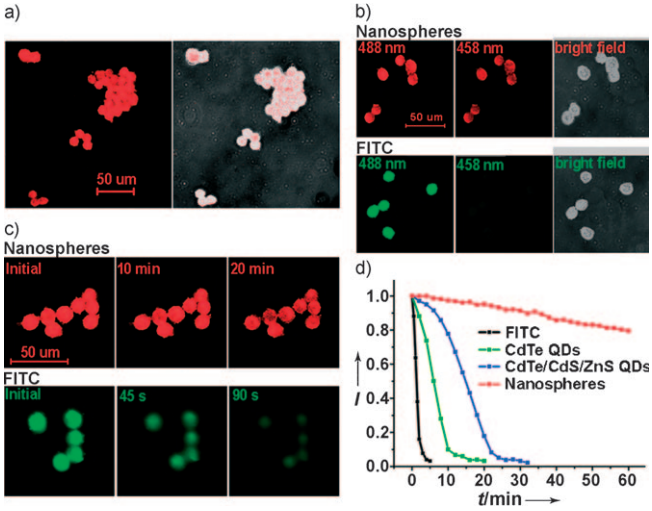

Figure 5. a) Fluorescence microscopy images of HEK2-293T cells labeled with the as-prepared nanospheres excited at 488 nm (left) and superposition of fluorescence and transillumination images (right). b) Comparison of fluorescent signals of HEK293T cells imaging with the nanospheres (top) and FITC (bottom) excited at different wavelengths. c) Temporal evolution of fluorescence of the HEK293T cells labeled with the as-prepared nanospheres (top) and FITC (bottom). The nanospheres and FITC were both excited at 488 nm by argon laser with 8 μs dwell time and ca. 15 mW power. d) Photostability comparison of fluorescent II/VI QDs (CdTe QDs and CdTe/CdS/ZnS core–shell–shell QDs) and the as-prepared nanospheres. All of the samples were continuously irradiated by a 450 W xenon lamp.

the cells labeled with the nanospheres can be distinctly observed upon excitation at different wavelengths. As shown in Figure 5b, HEK293T cells were well stained by the nanospheres at both excitation wavelengths of 458 and 488 nm, whilst the signals of HEK293T cells labeled with the traditional fluorescein isothiocyanate (FITC) dye were only visible upon excitation at 488 nm. This is because the traditional dyes have a narrow absorption spectrum, whereas the nanospheres have a broad absorption spectrum and quantum-size effect,[3,4] and thus can be excited at different wavelengths. The capacity for multiwavelength excitation is significant, because it enables the detection of fluorescent signals under different excitation wavelengths and provides versatility and convenience for bioapplications.

The functionalized nanospheres possess another significant advantage, that is, robust anti-bleaching, for use as cellular imaging labels. Figure 5c shows that the fluorescence of the nanosphere-labeled cells maintained almost the same intensity throughout the entire UV irradiation period of 10 min. While the intensity decreased slightly with longer scanning time, the nanospheres still maintained distinctly observable fluorescence signals after 20 min of UV irradiation. In contrast, the fluorescence signals of cells imaged with common FITC dyes disappeared in only 90 s because of severe photobleaching of the dyes. To further validate the excellent photostability of the nanospheres, we compared the photostability of the FITC dye, fluorescent II/VI QDs (well recognized as a photostable biological fluorescent probe), and the as-prepared nanospheres in a parallel experiment. Figure 5d shows that the fluorescence of the FITC dye quickly dropped below undetectable levels in only 3 minutes, while the CdTe QDs maintained 80% of the original fluorescence intensity. The fluorescence intensity of CdTe/CdS/ZnS core–shell–shell QDs also decreased below 50% after 15 minutes, and became negligible after 30 minutes. In striking contrast, the fluorescence intensity of the nanospheres was remarkably stable, decreasing only slightly under long-term UV irradiation and preserving more than 80% of the original intensity even after irradiation for 60 minutes. Thus, we conclude that the PAA polymer shell effectively protects the SiQDs from direct UV irradiation, and the photoluminescence of SiQDs,[18] which results in superior photostability compared to the fluorescent dyes and II/VI QDs. The nanospheres also possess favorable biocompatibility because of the noncytotoxicity of silicon. This was shown by 3-(4,5-dimethylthiazol-2-yl)-2,5-diphenyltetrazolium bromide (MTT) assays, which showed that the cell viability remained at roughly 100% after 24 h incubation of HEK293T cells with the same concentration of nanospheres as that used in the cellular imaging experiment. Furthermore, the nanospheres can conjugate with proteins since their surface hydroxy groups can readily react with the amino group of proteins by an EDC/Sulfo-NHS conjugation reaction (EDC = 1-ethyl-3-(3-dimethylaminopropyl)carbodiimide hydrochloride, Sulfo-NHS = *N*-hydroxysulfosuccinimide).[19]

In conclusion, a new class of silicon-based nanospheres of controllable sizes have been prepared following a novel strategy, which used theoretical calculations as a guide. Significantly, these nontoxic nanospheres possess good water dispersibility, high photoluminescence, and excellent photostability. Furthermore, cellular experiments indicate that the as-prepared nanospheres are remarkably efficacious for real-time and long-term cell imaging. The totality of the results suggests that the ultrastable and highly fluorescent nanospheres are promising candidates for cellular probes.

Received: May 13, 2008
Revised: September 19, 2008
Published online: October 31, 2008

Keywords: fluorescent probes · nanostructures · photostability · quantum dots · silicon

[1] X. Michalet, F. F. Pinaud, L. A. Bentolila, J. M. Tsay, S. Doose, J. J. Li, G. Sundaresan, A. M. Wu, S. S. Gambhir, S. Weiss, *Science* **2005**, *307*, 538–544.
[2] J. K. Jaiswal, H. Mattoussi, J. M. Mauro, S. M. Simon, *Nat. Biotechnol.* **2003**, *21*, 47–51.
[3] a) M. P. Bruchez, Jr., M. Moronne, P. Gin, S. Weiss, A. P. Alivisatos, *Science* **1998**, *281*, 2013–2016; b) W. C. W. Chan, S. Nie, *Science* **1998**, *281*, 2016–2018.
[4] J. M. Klostranec, W. C. W. Chan, *Adv. Mater.* **2006**, *18*, 1953–1964.

[5] a) I. L. Medintz, H. T. Uyede, E. R. Goldman, H. Mattoussi, *Nat. Mater.* **2005**, *4*, 435 – 446; b) X. Gao, Y. Y. Cui, R. M. Levenson, L. W. K. Chung, S. M. Nie, *Nat. Biotechnol.* **2004**, *22*, 969 – 976; c) S. J. Clarke, C. A. Hollmann, Z. J. Zhang, D. Suffern, S. E. Bradforth, N. M. Dimitrijevic, W. G. Minarik, J. L. Nadeau, *Nat. Mater.* **2006**, *5*, 409 – 417.
[6] N. Gaponik, D. V. Talapin, A. L. Rogach, K. Hoppe, E. V. Shevchenko, A. Kornowski, A. Eychmuller, H. Weller, *J. Phys. Chem. B* **2002**, *106*, 7177 – 7185.
[7] a) A. M. Derfus, W. C. W. Chan, S. N. Bhatia, *Nano Lett.* **2004**, *4*, 11 – 18; b) A. Hoshino, K. Fujioka, T. Oku, M. Suga, Y. F. Sasaki, T. Ohta, M. Yasuhara, K. Suzuki, K. Yamamoto, *Nano Lett.* **2004**, *11*, 2163 – 2169.
[8] a) C. Kirchner, T. Liedl, S. Kudera, T. Pellegrino, A. M. Javier, H. E. Gaub, S. Stolzle, N. Fertig, W. J. Parak, *Nano Lett.* **2005**, *5*, 331 – 338; b) S. T. Selvan, T. T. Tan, J. Y. Ying, *Adv. Mater.* **2005**, *17*, 1620 – 1625; c) V. A. Sinani, D. S. Koktysh, B. G. Yun, R. L. Matts, T. C. Pappas, M. Motamedi, S. N. Thomas, N. A. Kotov, *Nano Lett.* **2003**, *3*, 1177 – 1182.
[9] a) E. Chang, N. Thekkek, W. W. Yu, V. L. Colvin, R. Drezek, *Small* **2006**, *2*, 1412 – 1417; b) J. P. Ryman-Rasmussen, J. E. Riviere, N. A. Monteiro-Riviere, *Nano Lett.* **2007**, *7*, 1344 – 1348.
[10] a) W. S. Shi, H. Y. Peng, N. Wang, C. P. Li, L. Xu, C. S. Lee, R. Kalish, S. T. Lee, *J. Am. Chem. Soc.* **2001**, *123*, 11095 – 11096; b) D. D. D. Ma, C. S. Lee, F. C. K. Au, S. Y. Tong, S. T. Lee, *Science* **2003**, *299*, 1874 – 1877; c) F. A. Reboredo, E. Schwegler, G. Gall, *J. Am. Chem. Soc.* **2003**, *125*, 15243 – 15249.
[11] X. W. Zhao, O. Schoenfeld, S. J. Komuro, Y. Aoyagi, T. Sugano, *Phys. Rev. B* **1994**, *50*, 18654 – 18657.
[12] a) Z. F. Li, E. Ruckenstein, *Nano Lett.* **2004**, *4*, 1463 – 1467; b) J. H. Warner, A. Hoshino, K. Yamamoto, R. D. Tilley, *Angew. Chem.* **2005**, *117*, 4626 – 4630; *Angew. Chem. Int. Ed.* **2005**, *44*, 4550 – 4554.
[13] a) B. J. Eves, C. Y. Fan, G. P. Lopinski, *Small* **2006**, *2*, 1379 – 1384; b) B. J. Eves, G. P. Lopinski, *Langmuir* **2006**, *22*, 3180 – 3185.
[14] L. Q. Chu, W. J. Tan, H. Q. Mao, W. Knoll, *Macromolecules* **2006**, *39*, 8742 – 8746.
[15] a) Q. S. Li, R. Q. Zhang, T. A. Niehaus, Th. Frauenheim, S. T. Lee, *J. Chem. Theory Comput.* **2007**, *3*, 1518 – 1526; b) X. Wang, R. Q. Zhang, T. A. Niehaus, Th. Frauenheim, *J. Phys. Chem. C* **2007**, *111*, 2329 – 2400.
[16] Z. H. Kang, C. H. A. Tsang, Z. D. Zhang, M. L. Zhang, N. B. Wong, J. A. Zapien, Y. Y. Shan, S. T. Lee, *J. Am. Chem. Soc.* **2007**, *129*, 5326 – 5327.
[17] S. S. Banerjee, D. H. Chen, *Chem. Mater.* **2007**, *19*, 6345 – 6349.
[18] S. Godefroo, M. Hayne, M. Jivanescu, A. Stesmans, M. Zacharias, O. I. Lebedev, G. V. Tendeloo, V. V. Moshchalkov, *Nat. Nanotechnol.* **2008**, *3*, 174 – 178.
[19] S. P. Wang, N. Mamedova, N. A. Kotov, W. Chen, J. Studer, *Nano Lett.* **2002**, *2*, 817 – 822.
[20] J. N. Demas, G. A. Crosby, *J. Phys. Chem.* **1971**, *75*, 991 – 1024.
[21] a) Y. He, H. T. Lu, L. M. Sai, W. Y. Lai, Q. L. Fan, L. H. Wang, W. Huang, *J. Phys. Chem. B* **2006**, *110*, 13352 – 13356; b) Y. He, H. T. Lu, L. M. Sai, W. Y. Lai, Q. L. Fan, L. H. Wang, W. Huang, *J. Phys. Chem. B* **2006**, *110*, 13370 – 13374; c) Y. He, H. T. Lu, L. M. Sai, Y. Y. Su, M. Hu, Q. L. Fan, W. Huang, L. H. Wang, *Adv. Mater.* **2008**, *20*, 3416 – 3421.

